THE POWER ANALYSIS OF SEMICONDUCTOR DEVICES IN MULTI-PHASE TRACTION INVERTER TOPOLOGIES APPLICABLE IN THE AUTOMOTIVE INDUSTRY

Jakub Šimčák*, Michal Frivaldský, Patrik Resutík

Department of Mechatronics and Electronics, Faculty of Electrical Engineering and Information Technologies, University of Zilina, Zilina, Slovakia

*E-mail of corresponding author: jakub.simcak@uniza.sk

Jakub Simcak 0009-0000-9628-7752, Michal Frivaldsky 0000-0001-6138-3103,
Patrik Resutik 0000-0001-6643-4045

Resume

The article deals with the power analysis of semiconductor devices nowadays commonly used in perspective traction inverter topologies suitable for automotive industry applications. The power analysis is devoted to topologies, which are the Voltage Source Inverter (VSI) topology and perspective three-level alternatives, which are the Neutral Point Clamped (NPC) and T-type Neutral Point Clamped (T-NPC) traction inverter topologies. The main part of the power analysis of the proposed topologies is done on multi-phase versions (specifically six-phase). Mentioned topologies are modelled through the use of the simulation environment PLECS, while the focus is given on the accurate determination of semiconductor devices' power losses. Collected data of each analyzed topology are then processed using the MATLAB environment. The analysis of power parameters aims to find out which of the mentioned topologies achieves the highest efficiency as an VSI system at various power levels using the same input parameters.

Article info

Received 18 March 2024
Accepted 9 May 2024
Online 14 June 2024

Keywords:

multi-phase traction inverter
multi-level traction inverter
VSI
NPC
T-NPC
power loss analysis

Available online: https://doi.org/10.26552/com.C.2024.034

ISSN 1335-4205 (print version)
ISSN 2585-7878 (online version)

1 Introduction

At this moment, the sales of electrified vehicles are rising due to political support, battery technology improvements, growing charging infrastructure, and more and more new models from vehicle manufacturers. Electrification of the automotive industry is also spreading to new divisions of the road transport, which sets the new possible changes across the automotive industry. In the year 2022, electrified vehicles had a 14 % share of sales in the passenger cars category. This percentage number has risen every year since 2015, and it is predicted that this trend will continue. The global sales of electrified passenger cars in 2022 have grown by around 40 % compared to 2021. The largest share of the increase in global sales of electrified vehicles was recorded in China. Their global sales share doubled as compared to 2021 [1-4].

Due to targets for reaching the carbon neutrality in road transport by 2050, research on the new possible improvements is needed across the entire traction drive of electrified vehicles [5].

There are several traction inverters possibility to enhance the power parameters. A traction inverter is a part of the traction drive of electrified vehicles and there are several possible ways to improve its power parameters. Since the commonly used traction drive now uses, mostly IGBT (Insulated gate bipolar transistor) - based, two-level Voltage Source Inverter topology (one leg contains the half-bridge connection of the semiconductor switching devices) [2], which can be seen in Figure 1, the first possible change that occurs, which can improve the power parameters of the inverter, is to replace the IGBT with wide-bandgap (WBG) devices as SiC MOSFETs. These WBG devices have several advantages compared to Si IGBT. Operation at higher temperatures, higher breakdown voltages, lower switching losses at higher frequencies, and lower chip size are the reasons why Silicon Carbide (SiC) and Gallium Nitride (GaN) MOSFETs are suitable for IGBT

Table 1 *Common input parameters for all the analyzed traction inverter topologies*

Electrical variable/unit	value
DC-Link input voltage [V]	800
DC-Link capacitor [µF]	300
Switching frequency [kHz]	20
Continuous output power [kW]	10 - 100
Power factor [-]	0.75
Estimated efficiency [%]	98

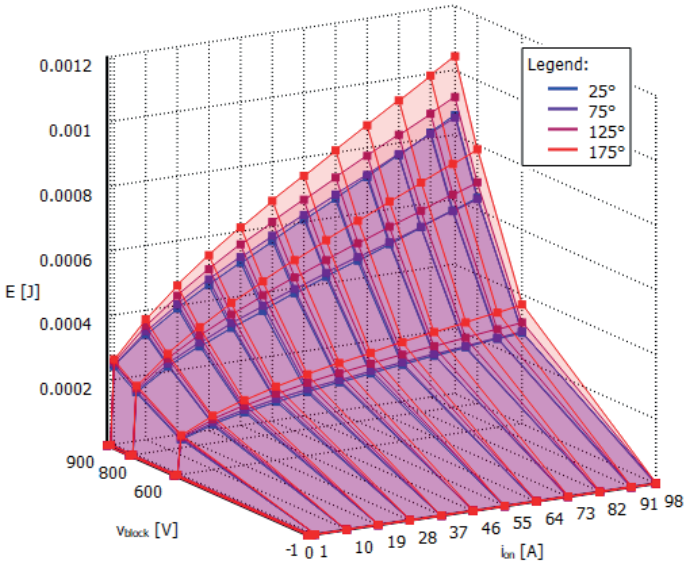

Figure 1 *Thermal model of the NTBG020N120SC1 - Turn on switching losses*

replacement [6-10].

Apart from that, there are other options for achieving the higher efficiency of the traction inverter. For example, a change in the number of phases of the traction inverter from three-phase drives to multi-phase ones. In the case of automotive traction drives, the closest development step would be six-phase drives. Multi-phase drives split the power into a higher number of phases, which means that the power ratings per phase are lower [4]. Improved current handling, enhanced fault tolerance, reduced DC-Link capacitor requirements, as well as modularity are the main strengths of the multiphase inverters [11-14].

Another possible traction drive enhancement is to change the two-level VSI topology with an alternative topology. Three-level inverters were, based on advanced studies, presented as the most viable alternative for the nowadays used VSI architecture. There were studies, that suggested that the two most competitive three-level topologies that have been developed are T-type Neutral Point Clamped (T-NPC) and Neutral Point Clamped (NPC). The efficiency of the VSI topology is higher than the mentioned two topologies only at lower switching frequencies than 10 kHz. At a higher switching frequency than 10, but lower than 30 kHz, T-NPC topology is expected to be more efficient, while at the higher switching frequencies than 30 kHz the NPC topology provides higher efficiency than both mentioned topologies. Apart from that the three-level topologies offer lower harmonic distortion of the output voltage and offer reduced requirements for the EMI filter. However, the volume of DC-Link capacitors is twice that big compared to the VSI topology. In addition, the costs of producing three-level inverters are higher and the control is more complex [15-18].

This study is devoted to analyzing the power losses of the semiconductor devices of the three-phase VSI, its six-phase version, and six-phase three-level topologies NPC and T-NPC, at the same power levels. The power analysis performed in the PLECS software deals with the power losses of the semiconductor switching devices, from which the all analyzed traction inverter topologies are composed. Output power parameters obtained from the analysis are compared to each other to investigate the highest efficiency of the traction inverter system topology.

2 Operational parameters of the simulation models of investigated VSI alternatives

All the analyzed topologies are built based on the same input parameters, semiconductor switching devices (ones that are directly connected to a DC-Link),

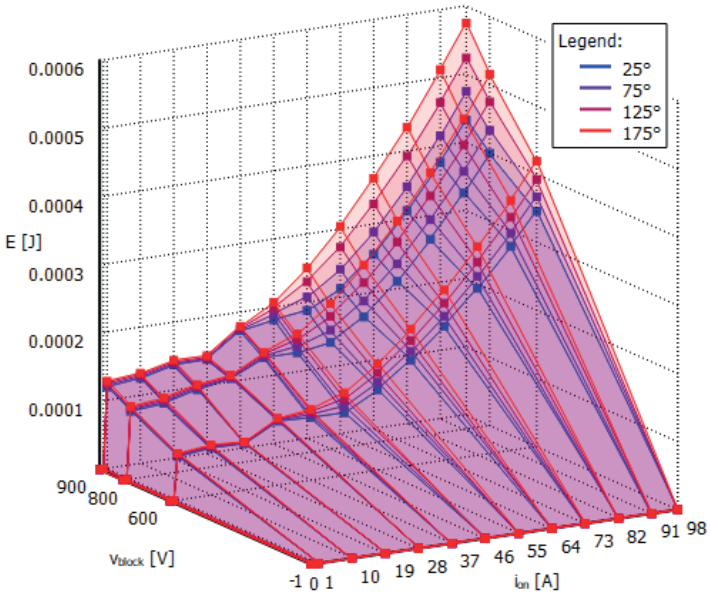

Figure 2 *Thermal model of the NTBG020N120SC1 - Turn-off switching losses*

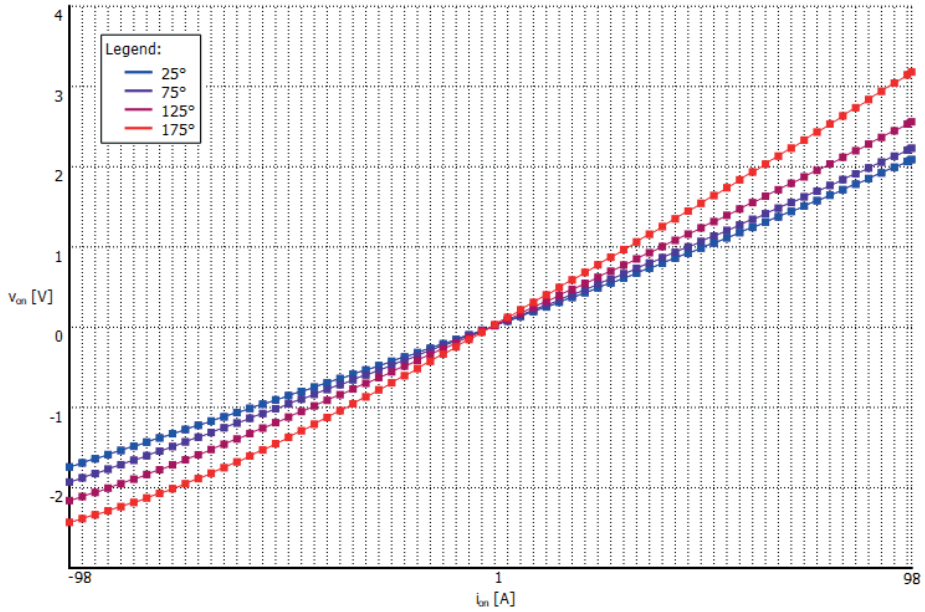

Figure 3 *Thermal model of the NTBG020N120SC1 - Conduction losses*

simulation model of the cooling system, control technique, and parameters of the AC load. The input parameters are shown in Table 1.

These input parameters were selected based on the literature that deals with future trends in automotive traction drive systems described in [3-5]. The value of the DC-Link capacitor was determined based on the calculations using the method mentioned in [7]. In all the proposed analyses of the topologies, discrete silicon carbide semiconductor devices from *onsemi* were used. To be able to reach the high-power levels, such as 100 kW, with the use of discrete packages of semiconductor devices, their parallel connection is necessary to be applied.

Based on the previous work with the PLECS simulation software, the power loss calculations using this software are considered accurate, which enables fast-analyzing power losses of any circuit, that contains semiconductor devices. Since the PLECS works with thermal modelling of the semiconductor devices, it is possible to analyze the power losses of each semiconductor device of each proposed traction inverter topology suitable for automotive applications. The example of the thermal model of the switching device used in majority of the analyzed topologies NTBG020N120SC1 SiC MOSFET by *onsemi* can be seen in Figure 1 to Figure 3.

Any other semiconductor device, used in power parameters analysis in PLECS, must have its thermal model. This is what the thermal models of all used semiconductor devices in the power parameters analysis look like. These thermal models can be created based on

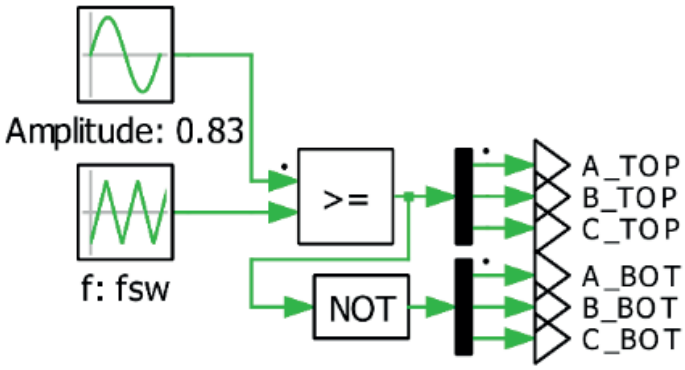

Figure 4 *Block scheme of the two-level three-phase SinePWM control technique*

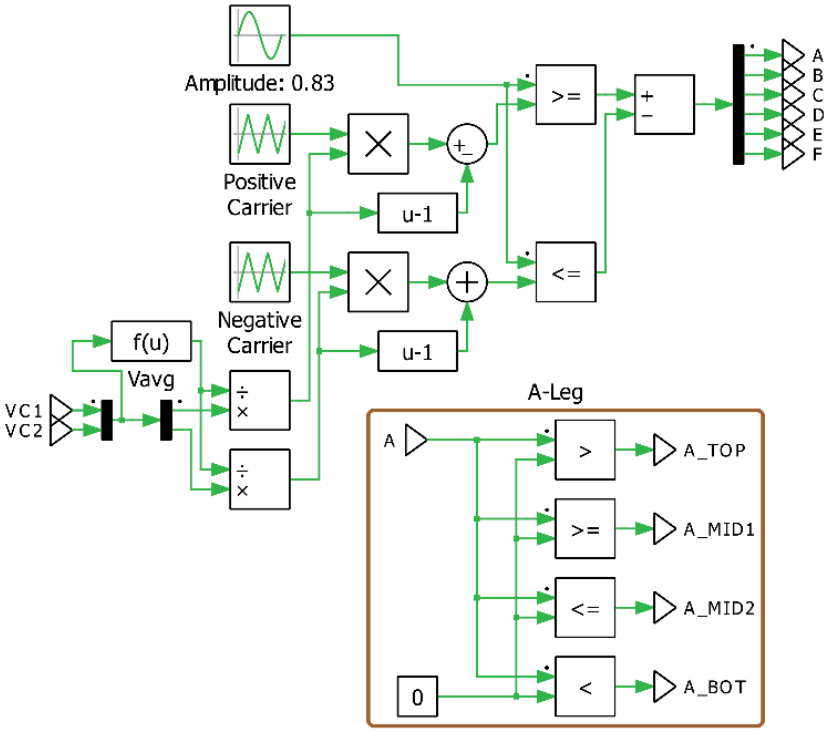

Figure 5 *Block scheme of the three-level six-phase SinePWM control technique with the example of comparison for each switching device*

the datasheet information, or some of the manufacturers nowadays offer these thermal models already created on their website or the PLECS website. Apart from the loss's waveforms, the PLECS thermal models contain information about the change of switching losses based on the change of the gate resistance or the thermal chain table.

Apart from the common input parameters, the used control technique, for all the analyzed topologies, is a sinusoidal pulse width modulation (SinePWM). It is because of its simplicity. The SinePWM control method is the most often used across the industry [19-21].

The block scheme of the two-level SinePWM, which is used as a control technique for the three-phase VSI topology analysis in PLECS can be seen in the block scheme in Figure 4. The same control technique, but modified to a three-level one, was used for the NPC and T-NPC topologies of the traction inverter. The block scheme of the modified SinePWM for three-level topologies can be seen in Figure 5, where the division algorithm for the A-Legs switching devices of the three-level inverter topology is also shown.

3 Power loss analysis of the traction inverter topologies simulation models

The analyzed topologies of the traction inverter suitable for automotive applications are the three-phase Voltage Source Inverter (nowadays commonly used across the automotive industry), its six-phase version, and the three-level six-phase topologies, which are NPC and T-NPC. These topologies were analyzed in PLECS, where based on the input parameters the power loss calculation was performed.

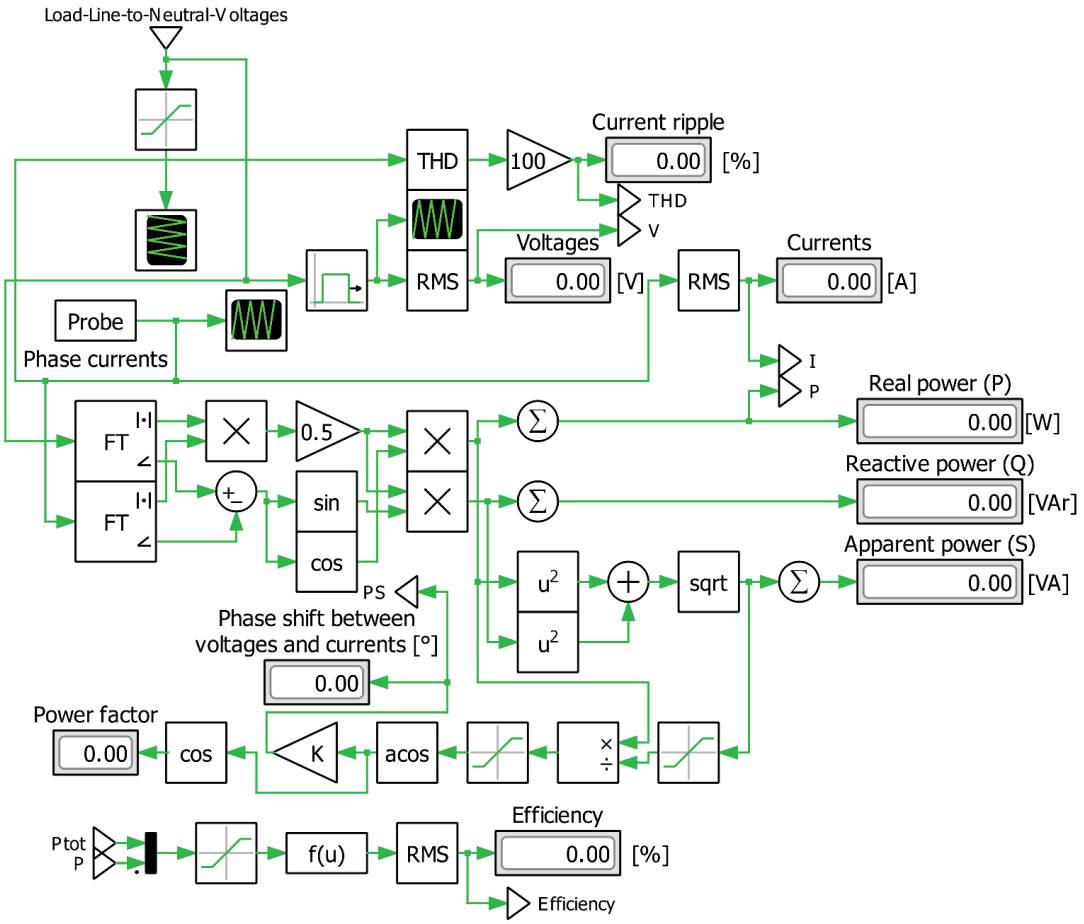

Figure 6 *Calculation scheme for the efficiency evaluation of the investigated VSI alternatives*

As it was mentioned in the previous section, SiC MOSFET NTBG020N120SC1 is used in the majority of analyzed topologies. This MOSFET blocking voltage is 1200 V. Since the selected input voltage is 800 V, the closest suitable power SiC MOSFET value of the blocking voltage category is 1200 V. MOSFETs with a blocking voltage of 900 V are also commercially available, but in order not to damage the given switching device with overvoltage, it is necessary to take into consideration a 20% margin of the blocking voltage, which at the value of the input voltage of 800 V is 160 V above its limit value. It means that these 900 V blocking voltage MOSFETs are not suitable for this application. The 1200 V blocking voltage switching device is used in both versions of the VSI topology and T-NPC as a switching device connected to the DC-Link (TOP and BOT ones).

The required blocking voltage level of the semiconductor devices used in the NPC topology is the half value of the DC-Link input voltage plus a 20% reserve. For this reason, 650 V blocking voltage MOSFETs NTBG015N065SC1 were selected. Their value of continuous drain current varies based on the temperature but even at 100 °C does not drop below 103 A. These MOSFETs are also used as a bipolar switch in the T-NPC topology.

The NPC topology also contains clamping Schottky diodes, which should be zero recovery ones. The voltage level of these diodes is the same as the MOSFETs. So, based on these key parameters of the clamping diodes, the FFSH5065B-F085 from *onsemi* was selected.

For the estimation of efficiency of individual VSI alternatives, the calculation scheme was used (Figure 6). As is seen from the figure, the circuit connection contains Fourier transformation blocks, in order to evaluate individual power components, i.e. the active power, reactive power and apparent power. Instead of evaluation of the total system efficiency, power factor is evaluated, as well. The power losses of the inverters are estimated for active and passive (filter components) devices of the main circuit, while built-in block of the simulation environment have been used (Switch Loss Calculator for power semiconductors and periodic averaging scheme for passive components).

3.1 The three-phase voltage source inverter topology

Voltage Source Inverter topology is commonly used topology in automotive traction inverters due to its reliability, robustness, and relatively high efficiency at lower costs [3].

A simulation model of the three-phase Voltage Source Inverter topology, assembled by the discrete

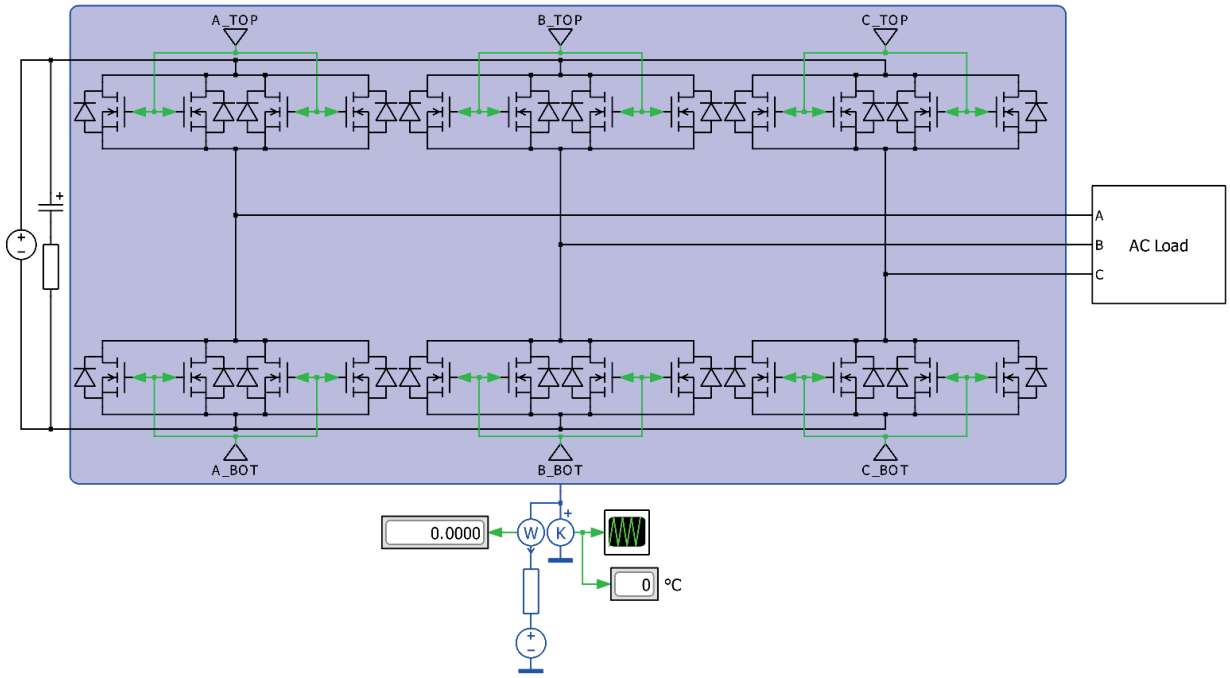

Figure 7 *Three-phase Voltage Source Inverter topology*

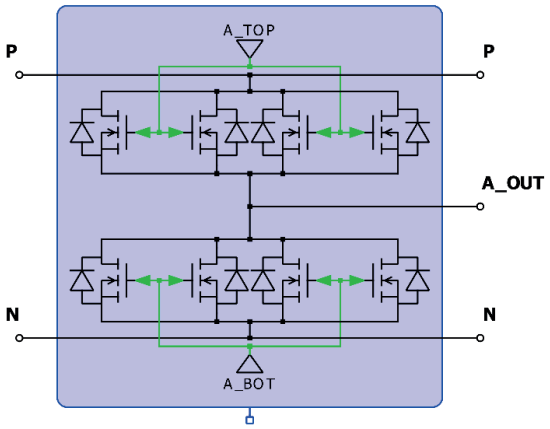

Figure 8 *A-Leg of the analyzed circuit of the three-phase VSI topology*

switching devices, is shown in Figure 7. The VSI topology consists of a half-bridge connection of two switching devices for each phase.

Figure 8 shows a closer look at the one phase of the three-phase VSI topology. As can be seen, one switch consists of four parallel connected NTBG020N120SC1 SiC MOSFETs to be able to reach the current requirements for the maximum of 100 kW output power, at an acceptable junction temperature of SiC MOSFETs (lower than 175 °C). At 20 kHz switching frequency, the RMS value of junction temperature of each parallel connected SiC MOSFET was at 74.4 °C. A parallel connection of the switching devices is needed because the maximum value of NTBG020N120SC1 continuous drain current is only 98 A, where the value is lowered by circa 20 A when the 20 % reserve rule is applied.

Before the power parameters analysis (determination of power loss values), it is important to verify the system's functionality. In Figure 9 and Figure 10. the output waveforms of line voltages and phase currents of the AC Load can be seen, which demonstrate the correct functionality of the three-phase VSI topology system. The RMS value of the AC load line-to-neutral voltage, at all power levels, was on average 234.39 V. The two-level character of the line-to-line voltages is easily observable in Figure 8. The AC load current RMS value at the highest power level (100 kW) was 190.18 A. As can be seen in Figure 9, the total harmonic distortion (THD) of the phase current is low. The value of the phase current THD, at all power levels, for the three-phase VSI topology is 0.19 %.

Power losses of the three-phase VSI topology at the different power levels are shown in Figure 11. In this figure, it can be noticed that at output power values lower than 30 kW, the switching losses form most of the total power losses. From the 30 kW conduction losses form most of the power losses. When using these semiconductor devices, the power losses reach

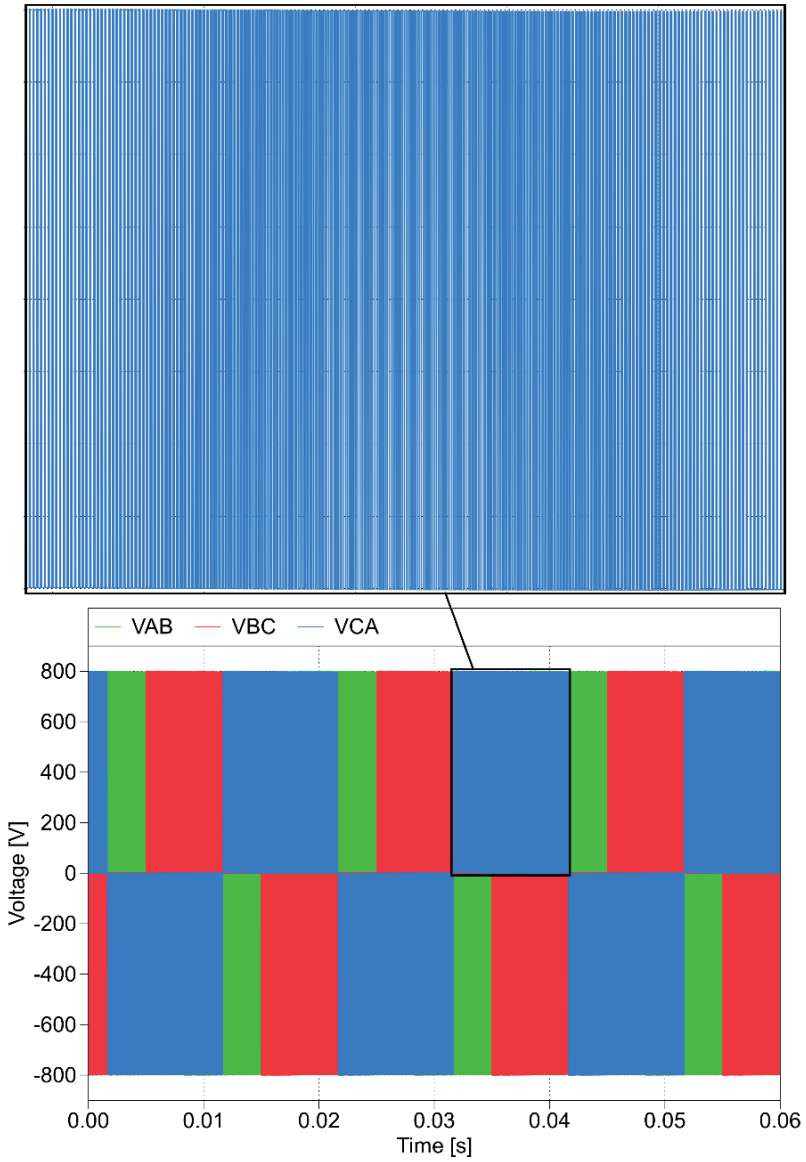

Figure 9 *Line-to-line voltage waveforms of the three-phase VSI at 100 kW output power*

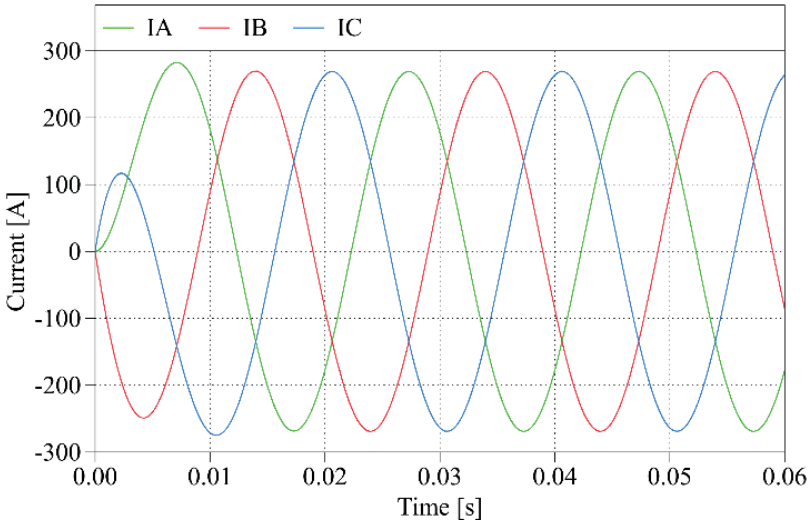

Figure 10 *Phase current waveforms of the three-phase VSI at 100 kW output power*

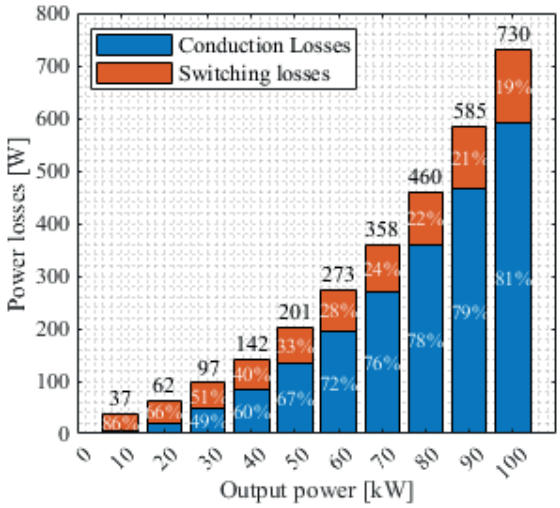

Figure 11 *Power losses of the three-phase VSI topology*

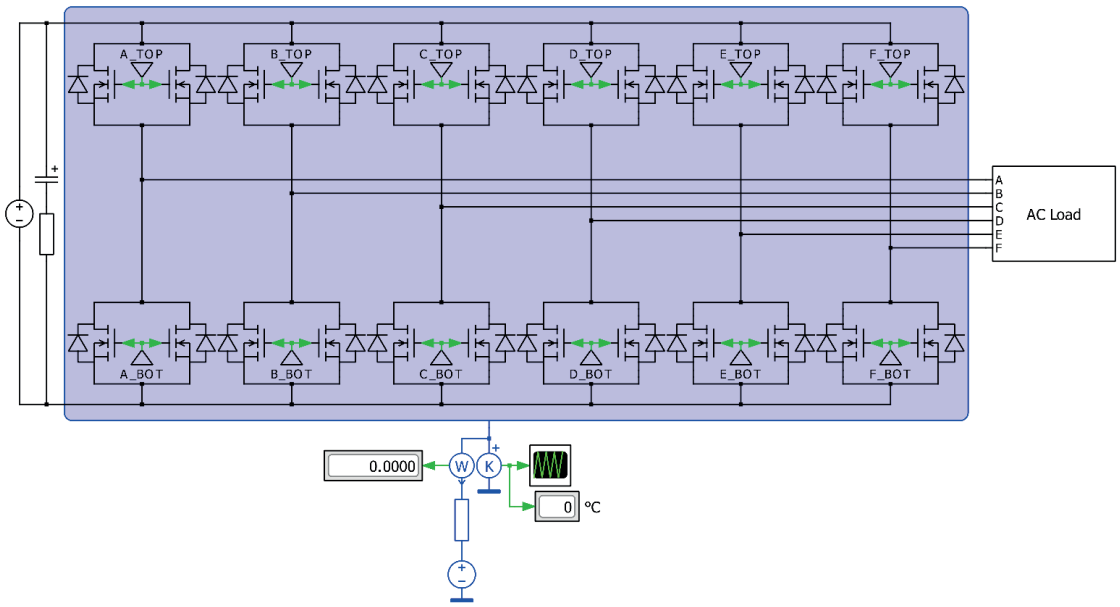

Figure 12 *The six-phase Voltage Source Inverter topology*

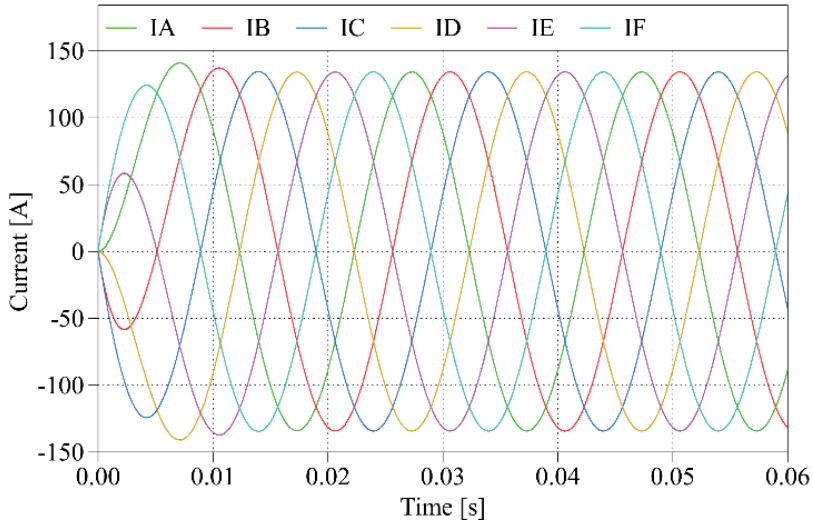

Figure 15 *Phase current waveforms of the six-phase VSI at 100 kW output power*

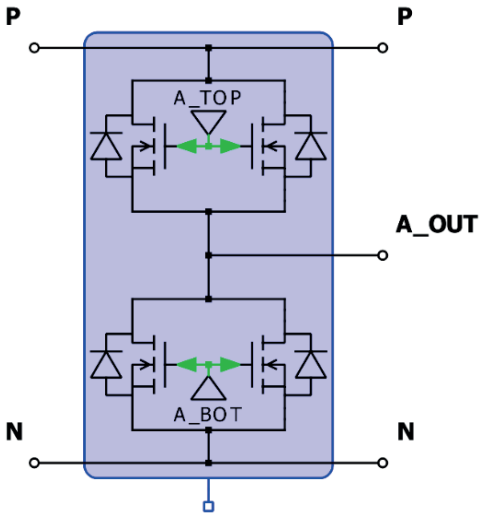

Figure 13 *A-Leg of the analyzed circuit of the six-phase VSI topology*

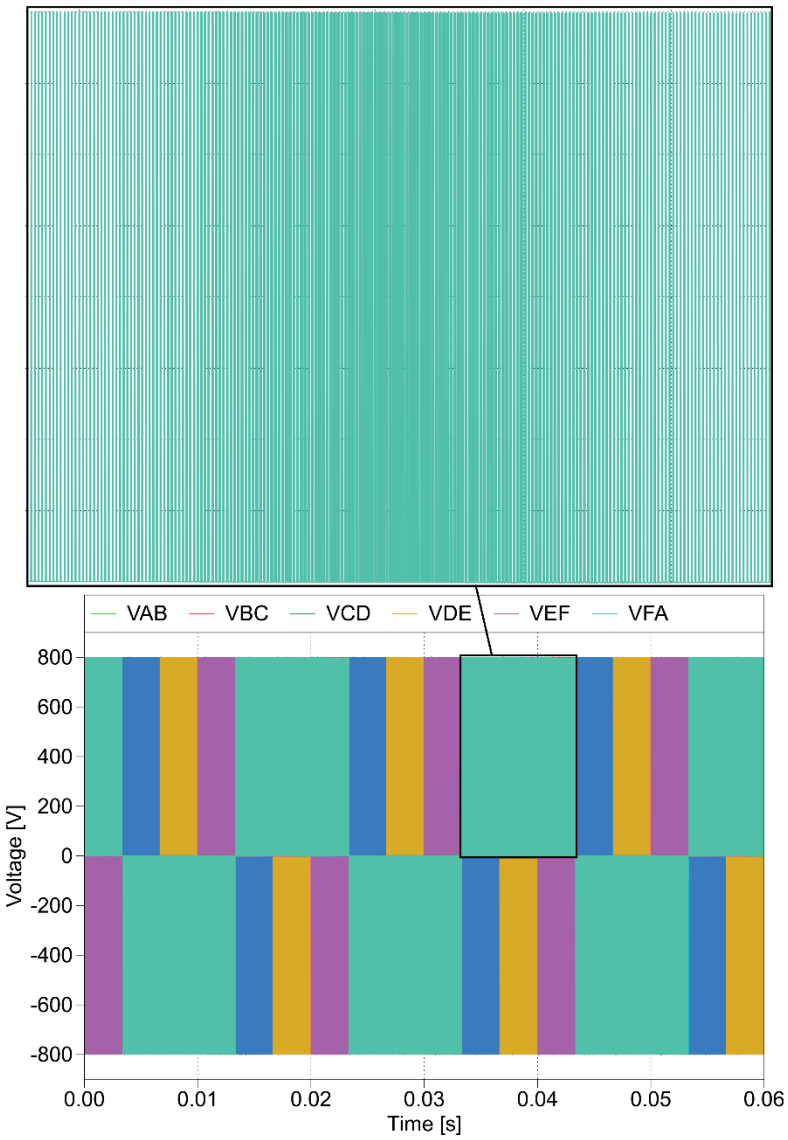

Figure 14 *Line-to-line voltage waveforms of the six-phase VSI at 100 kW output power*

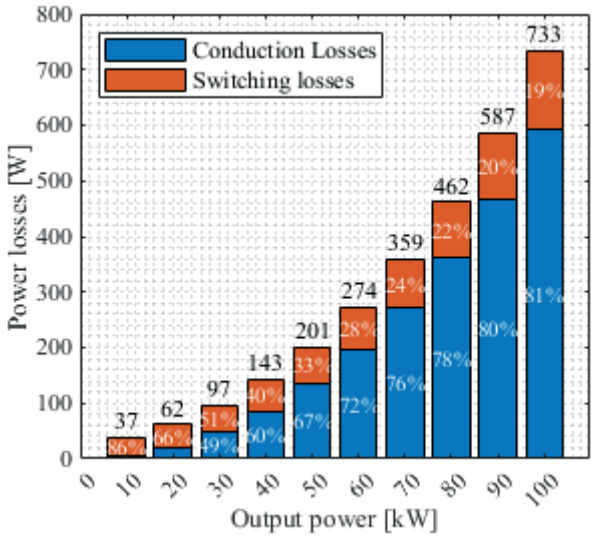

Figure 16 *Power losses of the six-phase VSI topology*

a maximum value of 730 W at a maximum output power of 100 kW.

These values of power losses are obtained when the temperature of the thermal domain is stable. The maximum temperature of the modelled heatsink reached a value of 61.5 °C at 100 kW.

3.2 The six-phase voltage source inverter topology

This topology (shown in Figure 12) is the same as the previous one, from the point of view of the configuration of the switching devices, but it is enhanced by the number of phases, which is doubled. This change was also made based on the future trends, which were mentioned in the section dedicated to input parameters of simulation models.

The multi-phase topologies have several advantages over the three-phase ones. One of them is, for example, half the phase current (which can be observed by comparing Figure 10 and Figure 15) or lower DC-Link current ripples, which lower the requirements for selection of a DC-Link capacitor [4].

Since the current requirements of the switching devices are lowered, the number of parallel connected SiC MOSFETs is also reduced. As shown in Figure 13, the one switching device contains two parallel connected SiC MOSFETs. The selection of switching semiconductor devices for this six-phase application was based on the same criteria as for the three-phase version, which means that the same MOSFETs with a blocking voltage of 1200 V are used. The junction temperature of each MOSFET is also almost the same as in the three-phase version, which is around 74.3 °C. All the analyzed topologies have almost the same values of the RMS line-to-neutral voltage (Figure 14) as was mentioned in the three-phase VSI topology subsection (on average 234.4 V). Since these first two topologies are the same apart from the number of phases, the character of the line-to-line voltage is the same, but the output phase current is significantly lower, as it was predicted to be.

In numbers, compared to the three-phase VSI topology the RMS value of the six-phase VSI topology's phase current at the highest power level (100 kW) is 94.94 A, which proves that the statement about half the phase current in a doubled number of phases is correct. The total harmonic distortion of the phase current of the six-phase VSI topology is also the same as for the three-phase version, around 0.19 %.

The power loss values at different power levels and stabilized heatsink temperatures, which are shown in Figure 16, are the almost same as the power losses of the three-phase one. That is because the number of semiconductor devices, their method of connection, and their use in these two analyzed circuits are the same. This fact means that the costs of both versions would be the same.

There is no difference between the two VSI topologies in the case of the stabilized temperature of the modeled heatsink. Both three-phase and six-phase topologies reached the maximal temperature of 61.5 °C.

3.3 The six-phase neutral point clamped topology

The first analyzed three-level topology is Neutral Point Clamped (shown in Figure 17). This topology uses the clamping diodes to connect the half-bridge outputs and neutral point, which generates an additional voltage level [8]. The three-level topologies were introduced as a possible successor of the VSI topology in the automotive industry, because of lower harmonic distortion, reduced demands of EMI filters, and improved motor efficiency. These are the superior features compared to the VSI topology. The disadvantages are that the volume of

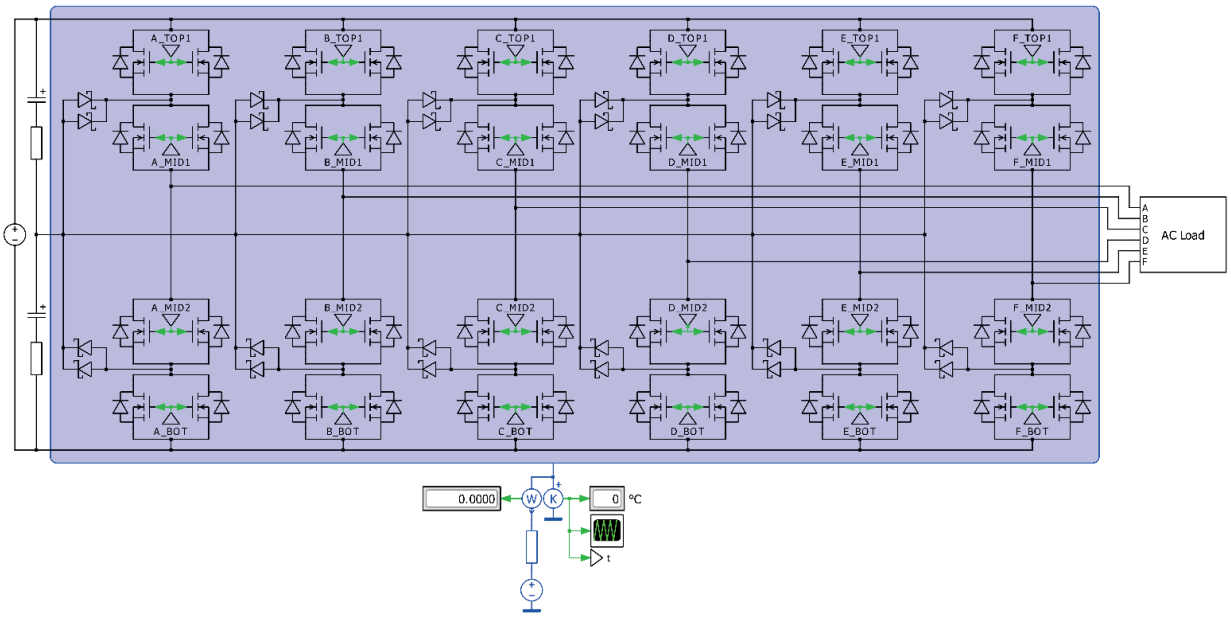

Figure 17 *The six-phase Neutral Point Clamped topology*

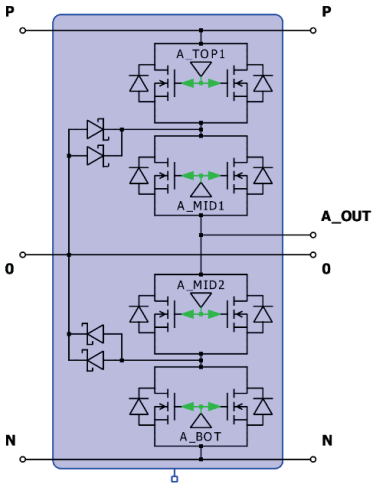

Figure 18 *A-Leg of the analyzed circuit of the six-phase NPC topology*

the DC-Link capacitor is doubled, and the number of semiconductor components is higher [3].

One phase of the NPC topology contains four switching devices and two clamping diodes. The voltage level compared to VSI topology is halved, which means that the demands on the blocking voltage of the switching devices, used in the NPC topology are reduced. A detailed look at one phase of this topology is displayed in Figure 18.

Two NTBG015N065SC1 MOSFETs, with a blocking voltage level of 650 V, are connected in parallel as one switching device, and two Schottky diodes FFSH5065B-F085 are connected in parallel as one clamping device. The junction temperature of each TOP and BOT MOSFET was 71.5 °C, each MID1 and MID2 one had a higher temperature of 2 °C, and the junction temperature of each Schottky diode was 77.4 °C.

As shown in Figure 19, compared to the two-level VSI topology the characteristics of the line-to-line voltage waveforms differ. As the category name of this topology implies, the character of the line-to-line voltage waveforms is enhanced to three levels.

The output line-to-line voltage and phase current waveforms of NPC topology at 100 kW are shown in Figure 19 and Figure 20. Despite the change in the characteristics of the line-to-line voltage waveforms, the output phase current remains unchanged and could be considered identical compared to the previously analyzed circuit (six-phase VSI). However, its total harmonic distortion is slightly higher compared to the mentioned VSI topology, at the level of 0.24%.

Power losses of the NPC topology contain apart from MOSFETs conduction and switching losses, the conduction losses of the diodes (Figure 21). These three categories make the total power losses of the NPC topology. Conduction losses of the clamping diodes make up a large part of the total power losses of the NPC topology, where at the maximum analyzed power

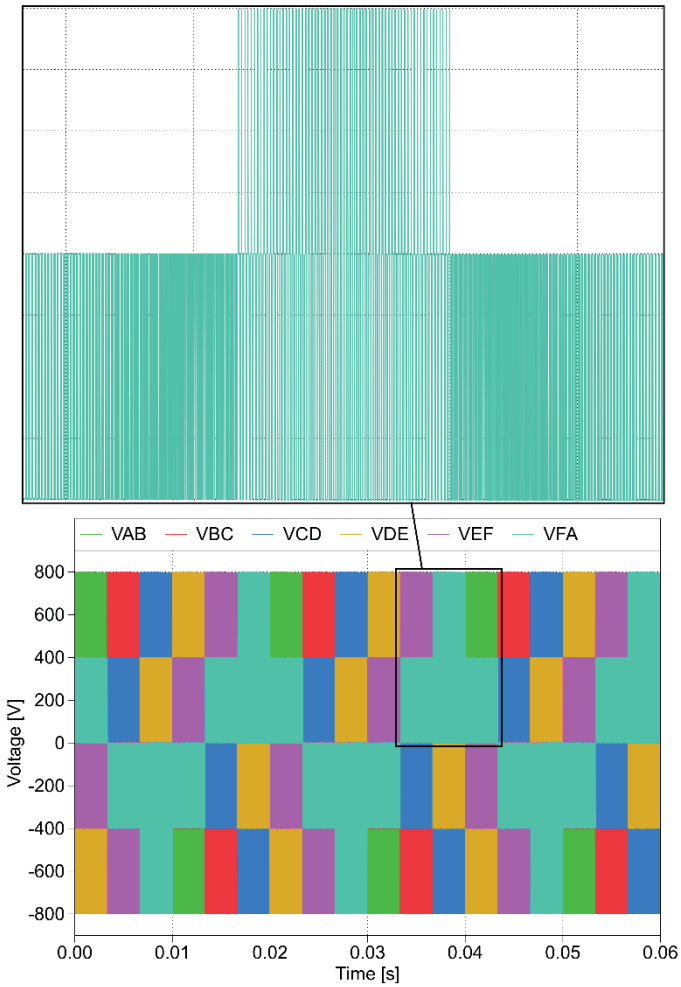

Figure 19 *Line-to-line voltage waveforms with closer look of VFA waveform of the six-phase NPC at 100 kW output power*

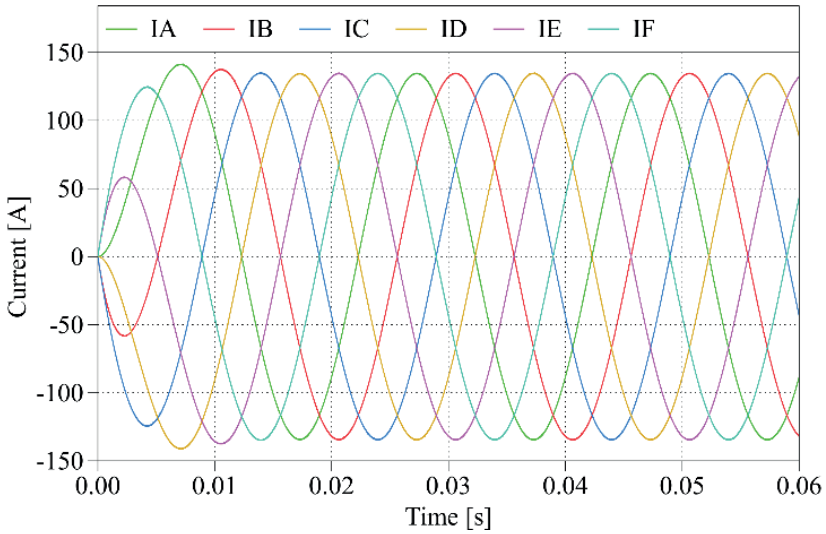

Figure 20 *Phase current waveforms of the six-phase NPC at 100 kW output power*

level of 100 kW their share is up to 41 %. Compared to the previously analyzed topologies, the total power loss values of the NPC topology, due to the conduction losses of the diodes, are higher. As it can be seen in Figure 21 the switching losses of the MOSFETs are much lower than the switching losses of rhe VSI topology MOSFETs. It creates just 3 % at the maximum of the total power losses of this topology.

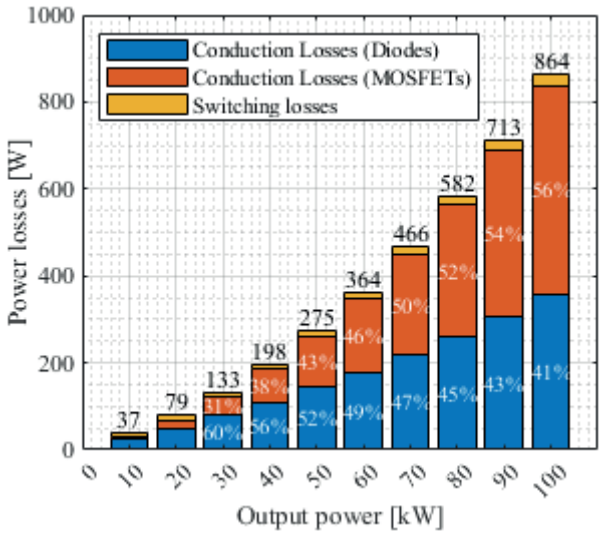

Figure 21 *Power losses of the six-phase NPC topology*

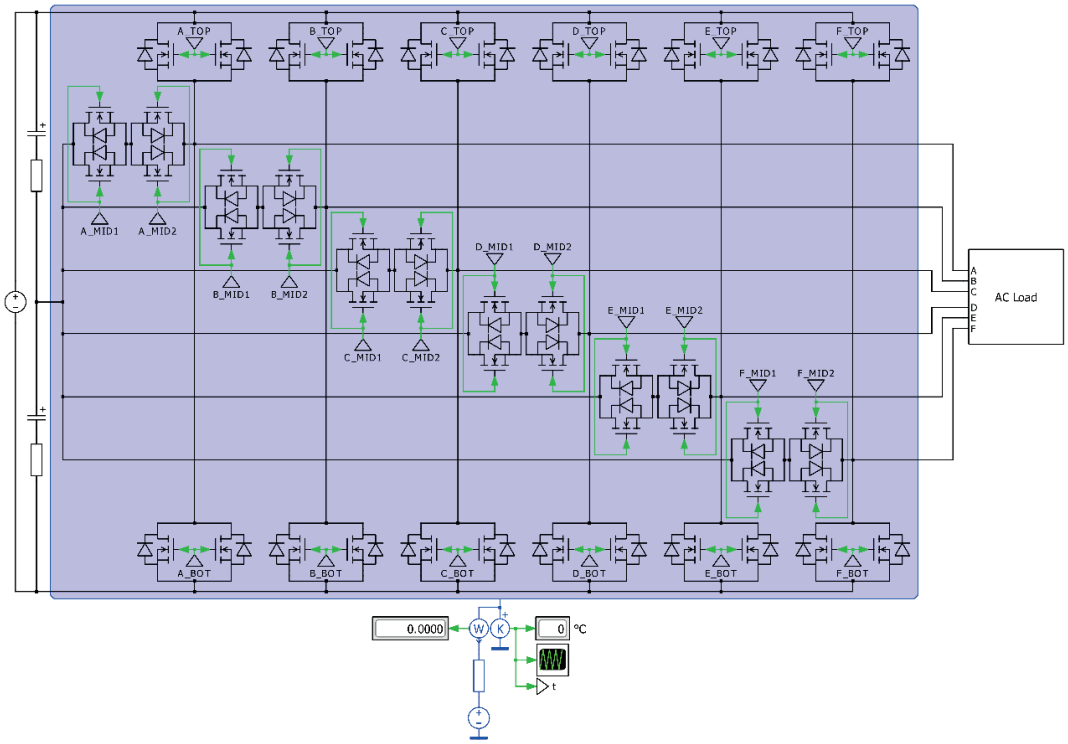

Figure 22 *The six-phase T-type Neutral Point Clamped topology*

The power losses were calculated at the stabilized modeled heatsink, with its maximum temperature at an output power of 100 kW of 68.2 °C, which is an increase of almost 7 °C compared to the VSI topology.

3.4 The six-phase T-type neutral point clamped topology

The last analyzed perspective automotive traction inverter topology is a three-level T-type Neutral Point Clamped topology. This topology's circuit can be seen in Figure 22.

The T-NPC topology is considered to be the most competitive solution for an automotive traction inverter. Compared to its three-level previously analyzed alternative, the number of semiconductor devices is lower, because of the clamping diodes absence. This results in the prediction that the power losses are expected to be lower than for the NPC topology. This three-level topology uses a bipolar switch as a connection between the output and neutral point. A close-up view of one phase of the T-NPC traction inverter topology is displayed in Figure 23.

The TOP and BOT in this topology are the switching devices with a 1200 V blocking voltage level. The

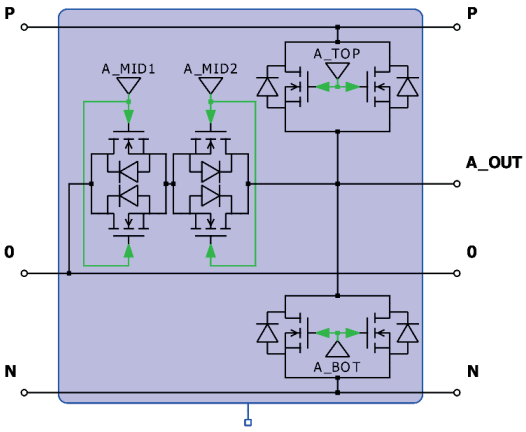

Figure 23 *A-Leg of the analyzed circuit of the six-phase T-NPC topology*

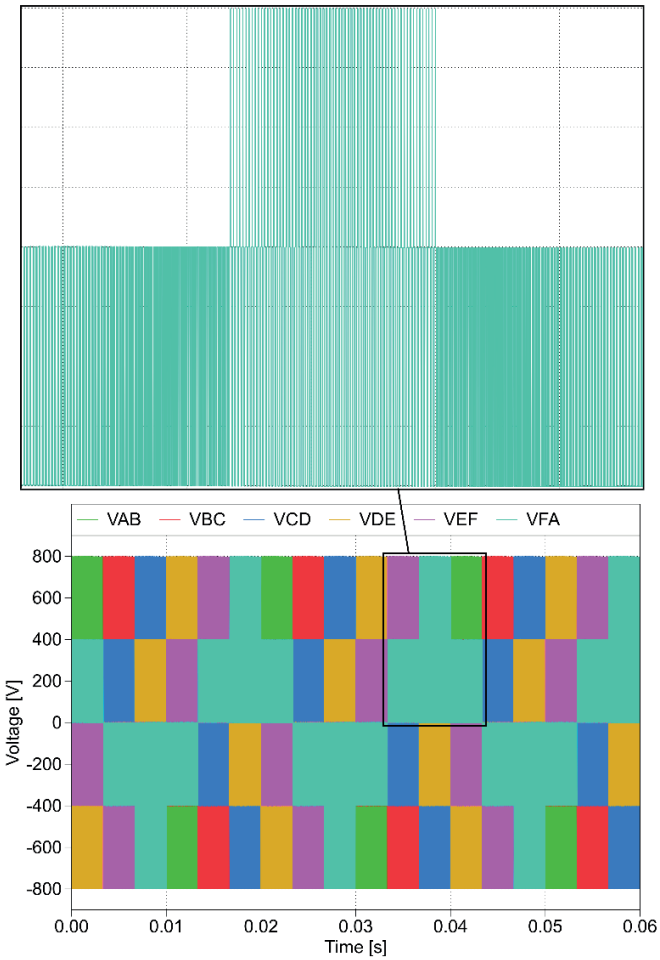

Figure 24 *Line-to-line voltage waveforms with closer look of VFA waveform of the six-phase T-NPC at 100 kW output power*

NTBG020N120SC1 as TOP and BOT MOSFETs are used. The bipolar switch (MID1 and MID2 MOSFETs) are built with the NTBG015N065SC1 which has a 650 V blocking voltage. For the same reason, as in the previously analyzed topologies, the switching device consists of two parallel connected MOSFETs. The junction temperature of each TOP and BOT MOSFET was 63.1 °C and for the bipolar switch MOSFETs (MID1 and MID2) it was 61.2 °C. These values are the lowest compared to all the other analyzed topologies at the maximum power level (100 kW). The output line-to-line voltage and phase current waveforms of NPC topology at 100 kW are shown in Figure 24 and Figure 25.

The output waveforms, with their parameters such as RMS values of line-to-neutral voltage or phase current of the T-NPC topology, are identical compared to the previously analyzed three-level topology.

The total power losses of the T-NPC topology are

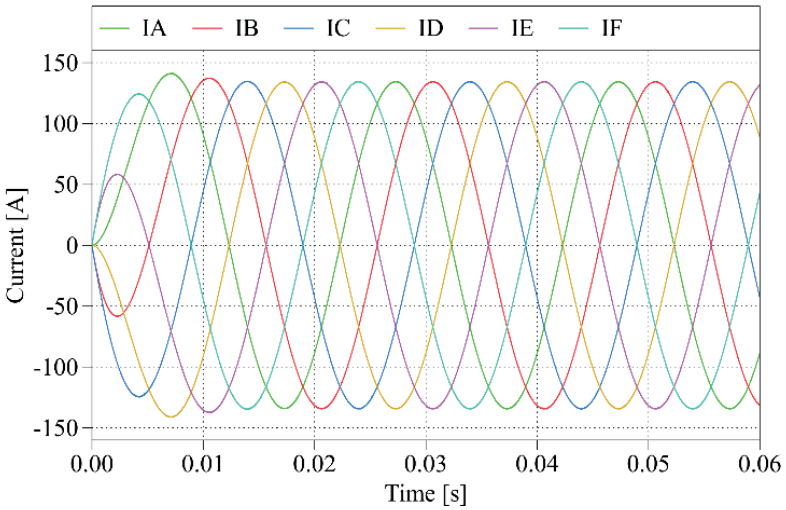

Figure 25 *Phase current waveforms of the six-phase T-NPC at 100 kW output power*

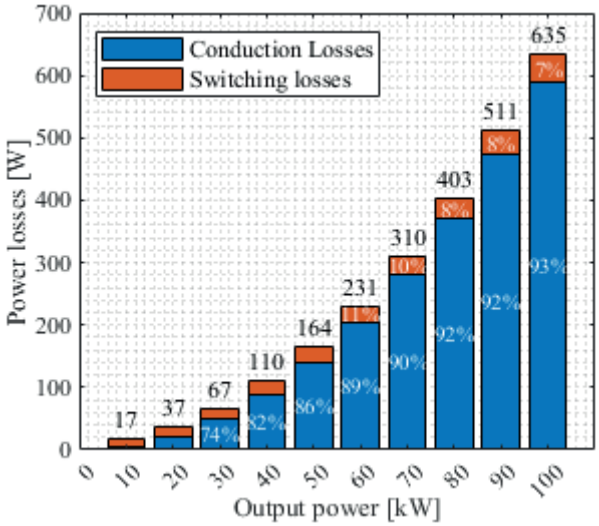

Figure 26 *Power losses of the six-phase T-NPC topology*

shown in Figure 26. These power losses are the lowest compared to all the other analyzed topologies. The three-level topologies are well known for their reduced switching losses. At the maximum power level of the analysis of T-NPC topology, the switching losses form only 7 % of the total 635 W power losses.

What makes this topology even superior to the other analyzed topologies, apart from the lowest power losses, is that the maximum value of the modeled heatsink temperature at the maximum power level reached 56.7 °C.

4 Efficiency evaluation of proposed traction inverter topologies

To be able to determine the best traction inverter topology suitable for automotive applications based on the power parameter analysis, it is necessary to express the efficiency of each topology at each power level. Based on the results of the total power losses of each analyzed traction inverter topology, the efficiency evaluation was performed.

The evaluation of the efficiency of each analyzed traction inverter topology is shown in Figure 27. The efficiency values at each power level of both analyzed versions of the VSI topology are the same. After analyzing these two versions of the VSI topology, it can be concluded that increasing the number of phases does not increase the efficiency of the traction inverter. However, the current requirements per phase, which are important when choosing the switching devices, and their involvement, were reduced. More specifically, the number of parallel connected switching devices were reduced, but the number of switching devices of the inverter stayed the same. The lowest reached efficiency was achieved by the NPC topology due to high power losses due to the high number of semiconductor devices (double the number of MOSFETs and additional clamping diodes compared to VSI topology), even

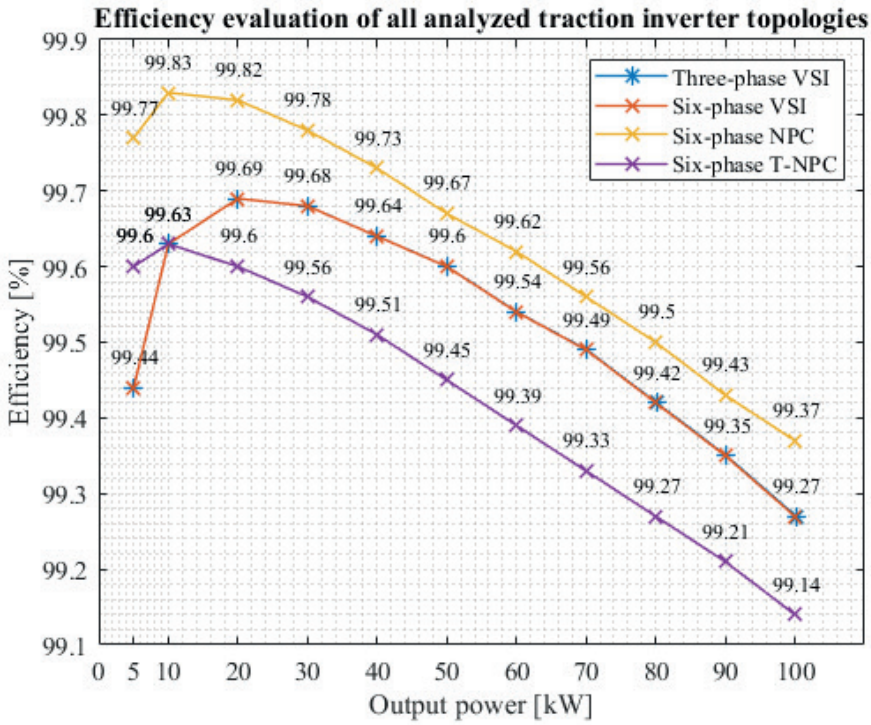

Figure 27 *Efficiency evaluation of all analyzed traction inverter topologies*

Table 2 *The costs of the analyzed traction inverter topologies*

Topology/Device	650 V MOSFET	1200V MOSFET	650V Diode	Cost of topology
3-ph VSI	0	24	0	$481.92
6-ph VSI	0	24	0	$481.92
6-ph NPC	48	0	24	$821.04
6-ph T-NPC	24	24	0	$843.84

though the switching losses were significantly reduced compared to both versions VSI topology. The most perspective topology for automotive applications based on the power parameters analysis is a three-level T-NPC topology. The number of switching devices of the six-phase T-NPC topology is doubled compared to the six-phase VSI topology, but the power losses are lower. This is mostly because of reduced switching losses.

These data on efficiencies of individual topologies at different power levels were built on the fact that the individual topologies were assembled using discrete WBG (SiC) devices. To achieve the maximum power of 100 kW, it was necessary to connect these devices in parallel, which increased the number of these devices in the circuit. Although the two-level topologies contained the same switching devices and in the same number, which was twice as low compared to the three-level ones, their achieved efficiency was not the highest at any power level. The three-level topologies contained twice the number of switching devices compared to the two-level VSI topology. However, only with the T-NPC topologies was the efficiency higher compared to the other analyzed topologies.

The device's pricing information is obtained from the official manufacturer's website. The costs of the whole topologies, which are determined in Table 2, were calculated based on the manufacturer's pricing stated on their official website, and the calculations were made only for the used semiconductor devices. The price per unit of the 650 V MOSFETs NTBG015N065SC1 was $15.08, the 1200 V MOSFETs NTBG020N120SC1 was $20.08, and 650 V Schottky diodes was $4.05. The price of these semiconductor devices is higher at retail stores.

The topology used nowadays in the automotive traction drives Voltage Source Inverter's cost is the lowest compared to the perspective alternative three-level topologies. The cost of the most efficient T-NPC topology is almost double the cost of VSI. These cost data are key to the practical implementation of traction drive's mass production of electrified vehicles. The higher the traction drive's efficiency, the longer the driving distance range of the electrified vehicle, and to achieve this, it would be necessary to enhance the traction inverter, for example by the change of switching devices from IGBTs to SiC MOSFETs, or the very topology of the connection of these devices. However, this comes at the expense of a higher price.

5 Conclusions

A description of the input parameters that were defined based on the automotive future trends for the power loss analysis of the semiconductor devices of traction inverter topologies suitable for automotive applications was determined. All the necessary parts of the thermal model of the semiconductor device, which is necessary for the power loss calculations, were created in PLECS, where the power loss analysis was performed. A closer look at sinusoidal PWM control algorithms was used for the two-level (VSI) and three-level (NPC and T-NPC) inverter topologies expressed by block diagrams. Before the actual analysis of the power losses, the selection procedure of discrete semiconductor devices that were used in the given topology was defined. For each of the analyzed topologies (VSI, NPC, and T-NPC) a simulation model was created in PLECS, the key properties of which were described. A close-up look at one phase of the inverter was displayed for each topology. The power loss analysis of all proposed topologies was performed at multiple power levels, but its line-to-line voltage and phase current waveforms were shown only at maximal power level. The results of the analysis of power losses were graphically displayed for each topology separately. The comparison of the analyzed topologies was based on the highest reached efficiency and on the costs of purchasing semiconductor devices.

It is seen from the results, that NPC converter exhibits the highest efficiency within the whole power range that was evaluated. Approximately 0.1% up to 0.3% efficiency value is higher compared to the other evaluated topologies, even the higher amount of switching devices is presented within the main circuit of the NPC converter compared to standard VSI converter. Another advantage of multilevel inverter is better quality of electrical variables, thus lowering the negative impact on the electrical machine operation. The design technique that is being described makes it possible to evaluate the outcomes of different operational trials and offers a quick and dependable way to investigate multi-phase, multi-level power converter topologies. The 6-phase T-NPC inverter (100 kW) laboratory prototype is presently being developed. More thorough and in-depth analysis of the efficiency estimation using various methods (mathematical calculations, simulations, and laboratory experiments) is intended to be provided in future studies.

Acknowledgment

The authors would like to thank to the National grant agency APVV for project funding APVV-20-0500 and to national grant agency Vega for project funding 1/0274/24.

Conflicts of interest

The authors declare that they have no known competing financial interests or personal relationships that could have appeared to influence the work reported in this paper.

References

[1] MCKERRACHER, C., O'DONOVAN, A., SOULOPOULOS, N., GRANT. A., LYU, J., MI, S., DOHERTY, D., FISHER, R., CANTOR, C., YANG, M., AMPOFO, K., SEKINE, Y., LEACH, A., STOIKOU, E., SHI, J., XU, P., MALO YAGUE, L., HARING, A., GEURTS, P., ADRIAENSSENS, CH., ABRAHAM, A. T., KAREER, K. Electric vehicle outlook 2023 [online]. Available from: https://about.bnef.com/electric-vehicle-outlook/

[2] GOLI, C. S., ESSAKIAPPAN, S., SAHU, P., MANJREKAR, M., SHAH, N. Review of recent trends in design of traction inverters for electric vehicle applications. In: 2021 IEEE 12th International Symposium on Power Electronics for Distributed Generation Systems PEDG: proceedings [online]. IEEE. 2021. eISBN 978-1-6654-0465-5, eISSN 2329-5767, p. 1-6. Available from: https://doi.org/10.1109/PEDG51384.2021.9494164

[3] WU, Y., MUSTAFEEZ-UL-HASSAN, LUO, F. Design and optimization of a modular multiphase drive for multiphase machines. In: 2023 IEEE Applied Power Electronics Conference and Exposition APEC: proceedings [online]. IEEE. 2023. eISBN 978-1-6654-7539-6, eISSN 2470-6647, p. 1423-1428. Available from: https://doi.org/10.1109/APEC43580.2023.10131621

[4] KESBIA, N., SCHANEN, J. -L., ALAWIEH, H., GARBUIO, L., AVENAS, Y. Design by optimization of multiphase inverter for electric vehicle drive. In: 2020 22nd European Conference on Power Electronics and Applications EPE'20 ECCE Europe: proceedings [online]. IEEE. 2020. eISBN 978-9-0758-1536-8. p. 1-8. Available from: https://doi.org/10.23919/EPE20ECCEEurope43536.2020.9215677

[5] BRAZHNIKOV, A. V., BELOZEROV, I. R. Non-traditional control and advantages of multiphase AC inverter drives. In: 2011 International Conference on Energy, Automation and Signal: proceedings [online]. IEEE. 2011. eISBN 978-1-4673-0136-7, p. 1-6. Available from: https://doi.org/10.1109/ICEAS.2011.6147207

[6] ARENA, G., AIELLO, G., SCELBA, G., CACCIATO, M., GENNARO, F. A cost-effective hardware in the loop implementation of dual active bridge for fast prototyping of electric vehicles charging controls. In:

2021 23rd European Conference on Power Electronics and Applications EPE'21 ECCE Europe: proceedings [online]. IEEE. 2021. eISBN 978-9-0758-1537-5, p. P.1-P.10. Available from: https://doi.org/10.23919/EPE21ECCEEurope50061.2021.9570652

[7] CHOLEWA, D., DROZDOWSKI, P. Simulink modeling of multiphase induction motors. In: 2018 14th Selected Issues of Electrical Engineering and Electronics WZEE: proceedings [online]. IEEE. 2018. eISBN 978-1-5386-8299-9, p. 1-6. Available from: https://doi.org/10.1109/WZEE.2018.8749007

[8] GLEISSNER, M., HARING, J., BAKRAN, M. -M., WONDRAK, W., HEPP, M., AG, M.-B. Advantageous fault-tolerant multilevel and multiphase inverter systems for automotive electric powertrains. In: 2020 Fifteenth International Conference on Ecological Vehicles and Renewable Energies EVER: proceedings [online]. IEEE. 2020. eISBN 978-1-7281-5641-5, p. 1-8. Available from: https://doi.org/10.1109/EVER48776.2020.9243131

[9] WANI, R., PATIL, S. L., SHINDE, P. Modeling and simulation of average current-mode controlled bidirectional multiphase dc-dc converters used in hybrid vehicles. In: 2021 6th International Conference for Convergence in Technology I2CT: proceedings [online]. IEEE. 2021. eISBN 978-1-7281-8876-8, p. 1-7. Available from: https://doi.org/10.1109/I2CT51068.2021.9418219

[10] REIMERS, J., DORN-GOMBA, L., MAK, C., EMADI, A. Automotive traction inverters: current status and future trends. *IEEE Transactions on Vehicular Technology* [online]. 2019, **68**(4), p. 3337-3350. ISSN 0018-9545, eISSN 1939-9359. Available from: https://doi.org/10.1109/TVT.2019.2897899

[11] SCHUCK, M., PILAWA-PODGURSKI, R. C. N. Ripple minimization through harmonic elimination in asymmetric interleaved multiphase DC-DC converters. *IEEE Transactions on Power Electronics* [online]. 2015, **30**(2), p. 7202-7214. ISSN 0018-9545, eISSN 1939-9359. Available from: https://doi.org/10.1109/TPEL.2015.2393812

[12] SALEM, A., NARIMANI, M. A review on multiphase drives for automotive traction applications. *IEEE Transactions on Transportation Electrification* [online]. 2019, **5**(4), p. 1329-1348. ISSN 0018-9545, eISSN 1939-9359. Available from: https://doi.org/10.1109/TTE.2019.2956355

[13] TAHA, W., AZER, P., CALLEGARO, A. D., EMADI, A. Multiphase traction inverters: state-of-the-art review and future trends. *IEEE Access* [online]. 2022, **10**, p. 4580-4599. eISSN 2169-3536. Available from: https://doi.org/10.1109/ACCESS.2022.3141542

[14] AULAGNIER, G., ABOUDA, K., ROLLAND, E., COUSINEAU, M., MEYNARD, T. Benefits of multiphase buck converters in reducing EME (electromagnetic emissions) analysis and application to on-chip converters for automotive applications. In: 2015 IEEE International Symposium on Electromagnetic Compatibility EMC: proceedings [online]. IEEE. 2015. eISBN 978-1-4799-6616-5, ISSN 2158-110X, eISSN 2158-1118, p. 102-107. Available from: https://doi.org/10.1109/ISEMC.2015.7256140

[15] CHEN, L., GE, B. High power traction inverter design and comparison for electric vehicles. In: 2018 IEEE Transportation Electrification Conference and Expo ITEC: proceedings [online]. IEEE. 2018. eISBN 978-1-5386-3048-8, p. 583-588. Available from: https://doi.org/10.1109/ITEC.2018.8450259

[16] ZAIDI, E., MAROUANI, K., BOUADI, H., NOUNOU, K., AISSANI, M., BENTOUHAMI, L. Control of a multiphase machine fed by multilevel inverter based on sliding mode controller. In: 2019 IEEE International Conference on Environment and Electrical Engineering and 2019 IEEE Industrial and Commercial Power Systems Europe EEEIC / I&CPS Europe: proceedings [online]. IEEE. 2019. eISBN 978-1-7281-0653-3, p. 1-6. Available from: https://doi.org/10.1109/EEEIC.2019.8783559

[17] BUTT, O. M., BUTT, T. M., ASHFAQ, M. H., TALHA, M., RAIHAN, S. R. S., HUSSAIN, M. Simulative study to reduce DC-link capacitor of drive train for electric vehicles. *Energies* [online]. 2022, **15**(12), 4499. eISSN 1996-1073. Available from: https://doi.org/10.3390/en15124499

[18] RODRIGUEZ, J., BERNET, S., STEIMER, P. K., LIZAMA, I. E. A survey on neutral-point-clamped inverters. *IEEE Transactions on Industrial Electronics* [online]. 2010, **57**(7), p. 2219-2230. ISSN 0278-0046, eISSN 1557-9948. Available from: https://doi.org/10.1109/TIE.2009.2032430

[19] PADMANABAN, S., WHEELER, P., BLAABJERG, F., ERTAS, A. H., OJO, J. O., SZCZESNIAK, P. Proposed novel multiphase-multilevel inverter configuration for open-end winding loads. In: 2016 18th European Conference on Power Electronics and Applications EPE'16 ECCE Europe: proceedings [online]. IEEE. 2016. eISBN 978-9-0758-1524-5, p. 1-9. Available from: https://doi.org/10.1109/EPE.2016.7695537

[20] BOTTARO, E., CACCIATO, M., RAFFA, A., RIZZO, S. A., SALERNO, N., VENEZIANO, P. P. Development of a SPICE modelling strategy for power devices in GaN technology. In: 47th Annual Conference of the IEEE Industrial Electronics Society IECON 2021: proceedings [online]. IEEE. 2021. eISBN 978-1-6654-3554-3, eISSN 2577-1647, p. 1-6, Available from: https://doi.org/10.1109/IECON48115.2021.9589710

[21] KYSLAN, K., LACKO, M., FERKOVA, Z., ZASKALICKY, P. V/f control of five phase induction machine implemented on DSP using Simulink coder. In: 2020 ELEKTRO: proceedings [online]. IEEE. 2020. eISBN 978-1-7281-7542-3, p. 1-6. Available from: https://doi.org/10.1109/ELEKTRO49696.2020.9130358